

Geophysical Research Letters[®]



RESEARCH LETTER

10.1029/2023GL102828

Key Points:

- Föhn and katabatic winds (downslope winds) and associated surface melt are prominent features on the Greenland and Antarctic ice sheets
- Surface melt trends associated with downslope winds have increased on the Greenland ice sheet and decreased on the Antarctic ice sheet

Supporting Information:

Supporting Information may be found in the online version of this article.

Correspondence to:

M. K. Laffin,
mlaffin@uci.edu

Citation:

Laffin, M. K., Zender, C. S., van Wessem, M., Noël, B., & Wang, W. (2023). Wind-associated melt trends and contrasts between the Greenland and Antarctic ice sheets. *Geophysical Research Letters*, 50, e2023GL102828. <https://doi.org/10.1029/2023GL102828>

Received 3 MAR 2023
Accepted 12 JUN 2023

Author Contributions:

Conceptualization: Matthew K. Laffin, Charles S. Zender, Wenshan Wang
Data curation: Melchior van Wessem, Brice Noël, Wenshan Wang
Formal analysis: Matthew K. Laffin
Methodology: Matthew K. Laffin, Charles S. Zender, Wenshan Wang
Supervision: Charles S. Zender
Visualization: Matthew K. Laffin
Writing – original draft: Matthew K. Laffin
Writing – review & editing: Matthew K. Laffin, Charles S. Zender, Melchior van Wessem, Brice Noël, Wenshan Wang

Wind-Associated Melt Trends and Contrasts Between the Greenland and Antarctic Ice Sheets

Matthew K. Laffin¹ , Charles S. Zender^{1,2} , Melchior van Wessem³, Brice Noël³, and Wenshan Wang¹ 

¹Department of Earth System Science, University of California Irvine, Irvine, CA, USA, ²Department of Computer Science, University of California Irvine, Irvine, CA, USA, ³Institute for Marine and Atmospheric Research Utrecht (IMAU), Utrecht University, Utrecht, The Netherlands

Abstract Föhn and katabatic winds (downslope winds) can increase ice sheet surface melt, run-off, and ice-shelf vulnerability to hydrofracture and are poorly constrained on the Greenland and Antarctic ice sheets (GIS and AIS). We use regional climate model simulations of the GIS and AIS to quantify and intercompare trends in downslope winds and associated melt since 1960. Results reveal surface melt associated with downslope wind is significant on both the GIS and AIS representing $27.5 \pm 4.5\%$ and $19.7 \pm 3.8\%$ of total surface melt respectively. Wind-associated melt has decreased $31.8 \pm 5.3\%$ on the AIS while total melt decreased $15.4 \pm 2.4\%$ due to decreased föhn-induced melt on the Antarctic Peninsula and increasing stratospheric ozone. Wind-associated melt has increased $10.3 \pm 2.5\%$ on the GIS, combining with a more positive North Atlantic Oscillation and warmer surface to increase total melt $34 \pm 5.8\%$.

Plain Language Summary Föhn and katabatic winds (wind that travels downslope) can increase ice sheet surface melt that increases sea levels and ice-shelf vulnerability. We use regional climate model simulations of the Greenland and Antarctic (GIS and AIS) to identify trends in downslope winds and associated melt since 1960. Results reveal surface melt associated with downslope winds is significant on both the GIS and AIS representing $27.5 \pm 4.5\%$ and $19.7 \pm 3.8\%$ of total surface melt respectively. Wind-associated melt has decreased $31.8 \pm 5.3\%$ on the AIS while total melt has decreased $15.4 \pm 2.4\%$ due to decreased föhn-induced melt on the Antarctic Peninsula and increasing stratospheric ozone that decreases sunlight at the surface. Wind-associated melt has increased $10.3 \pm 2.5\%$ on the GIS, combining with warmer surface temperatures to increase total melt $34 \pm 5.8\%$.

1. Introduction

The Greenland (GIS) and Antarctic ice sheets (AIS) hold enough water to raise global sea levels by 65.4 m (GIS 7.4 m, AIS 58 m) and have already contributed 18.4 mm (GIS 10.8 ± 0.9 mm, AIS 7.6 ± 3.9 mm) to global sea level rise since 1992 (Hanna et al., 2013; Rignot et al., 2008; The IMBIE team, 2018, 2020). Recent mass loss from the GIS has been primarily attributed to surface melt and runoff due to warmer air temperatures (Fettweis et al., 2017; Noël et al., 2019; Straneo & Heimbach, 2013) and increased insolation due to reduced summer cloud cover (Fettweis et al., 2017; Hofer et al., 2017; Noël et al., 2019; Tedesco et al., 2013). Mass loss from the AIS has been attributed to increased surface runoff and acceleration of marine-terminating glaciers primarily from regional increased air and ocean temperatures that have caused thinning, retreat, and collapse of marine-terminating glaciers and ice shelves (Auger et al., 2021; Bozkurt et al., 2020; Konrad et al., 2018; Rignot et al., 2004, 2014; Scambos et al., 2004). Surface melt and subsequent runoff are responsible for more than 80% of mass loss acceleration since the 1990s on the GIS (Andersen et al., 2015; Enderlin et al., 2014; Fettweis et al., 2017), and contribute to decreased ice shelf stability and collapse on ice shelves surrounding the AIS, which help to buttress grounded ice (Laffin et al., 2022; Massom et al., 2018).

Directionally consistent katabatic winds on the margins of the GIS and AIS, and föhn winds in the Antarctic Peninsula (AP) and northwestern Greenland, enhance surface melt rates (Datta et al., 2019; Laffin et al., 2021, 2022; Lenaerts et al., 2017; Mattingly et al., 2023; Wang et al., 2021). Katabatic winds originate in the cold, high, and dry ice sheet interior where relatively dense surface air drains downslope toward warmer regions. The polar highs coupled with the very cold and sloped ice sheets, make katabatic winds a consistent force on both ice sheet margins and some of the strongest and most persistent winds on Earth (Bromwich, 1988; Parish &

© 2023. The Authors.

This is an open access article under the terms of the [Creative Commons Attribution License](https://creativecommons.org/licenses/by/4.0/), which permits use, distribution and reproduction in any medium, provided the original work is properly cited.

Cassano, 2003). Föhn winds form when relatively cool moist air, forced over a mountain barrier, releases latent heat and precipitates during ascent. The warmer, drier air descends the leeside slope and compresses to create warm and dry gusty winds (Elvidge and Renfrew (2015)). Both katabatic and föhn wind mechanisms reduce atmospheric moisture and inhibit cloud formation which increases surface insolation and heating (Mioduszewski et al., 2016; Vihma et al., 2011). These strong winds turbulently mix the stable polar boundary layer, enhance sensible heat exchange, and accelerate surface melt (King et al., 2017; Kuipers Munneke et al., 2018; Laffin et al., 2021; Nylén et al., 2004; Vihma et al., 2011; Wang et al., 2021).

The effect of föhn and katabatic winds, which we will call downslope winds unless specified, on surface processes has been studied extensively on the AIS and through local case studies on the GIS. Observational and model studies have identified impacts of downslope winds on surface temperatures (Nylan et al., 2004; Parish and Bromwich, 1986), the surface energy budget (Kuipers Munneke et al., 2012, 2018; Laffin et al., 2021; Le Toumelin et al., 2021), surface mass balance including enhanced surface melt (Kuipers Munneke et al., 2012, 2018; Laffin et al., 2021; Mattingly et al., 2023; Wang et al., 2021), coastal precipitation (Grazioli et al., 2017), snow mass transport (Grazioli et al., 2017; Palm et al., 2017), ice shelf stability (Laffin et al., 2022), and sea ice and polynya formation with attendant impacts on ocean currents and biological productivity (Cape et al., 2014; Davis & Mcnider, 1997; Wenta & Cassano, 2020). Additionally, winds faster than 5–8 m/s can cause blowing snow that reflects shortwave radiation and enhances sublimation that limit surface melt (Grazioli et al., 2017; Le Toumelin et al., 2021), or expose bare ice that triggers the snow-ice albedo feedback (Lenaerts et al., 2017).

Despite this research, the contribution of downslope wind-associated melt compared to total melt, extent to which downslope wind regimes have changed, and how those changes have affected total melt and melt trends remain unclear. Here we use regional climate model simulations of the GIS from 1961 to 2019 and AIS from 1981 to 2019 to quantify melt associated with downslope winds, and estimate/explore how the wind regimes on each ice sheet have changed since the beginning of the simulation period. Section 2 describes the data and methods. Section 3 summarizes the total melt, mechanisms for melt, and melt trends associated with downslope winds. Section 4 summarizes the main findings and discusses the implications of the study in relation to the current understanding of surface melt on the GIS and AIS.

2. Data and Methods

2.1. Regional Atmospheric Climate Model Simulations (RACMO2)

We base our GIS and AIS analysis on 3-hourly output from simulations by the Regional Atmospheric Climate Model version 2.3p2 (RACMO2.3p2), with a horizontal resolution of 5.5 km (0.05°) focused on the GIS from 1961 to 2019, and 27.5 km (0.25°) focused on the AIS from 1981 to 2019. RACMO2 uses the physics package CY33r1 of the European Centre for Medium-Range Weather Forecasts-Integrated Forecast System (ECMWF-IFS, 2009) in combination with atmospheric dynamics of the High-Resolution Limited Area Model (HIRLAM). When compared with Automatic Weather Stations (AWS) observations of surface air temperature on the AP, AIS periphery, and the entire GIS, RACMO2 has a slight warm bias (0.7°C), and over/under-estimates downwelling shortwave/longwave radiation (9–24 W m²) due to underestimation of clouds and moisture but overall reproduces surface observations (Bozkurt et al., 2020; King et al., 2017; Laffin et al., 2021; Noël et al., 2018). RACMO2 is forced at the lateral boundaries with ERA-Interim data (Hersbach et al., 2020) and shows improvement in the surface energy fluxes and near-surface temperature from previous versions compared with AWS observations on both ice sheets (Bozkurt et al., 2020; Van Wessem et al., 2018).

2.2. Downslope Wind Detection

We associate downslope winds with melt that occurs when the wind direction is aligned with the topography surface slope (including Coriolis force) while surface melt occurs. We identify downslope winds on the GIS when the wind direction is within -10° to the left and 60° to the right of the downslope direction. The Coriolis force can steer downslope flow in the northern hemisphere to the right by up to 60° (Parish & Cassano, 2003; Van den Broeke & Van Lipzig, 2003; Wenta & Cassano, 2020; Wang et al., 2021). Mesoscale meteorological pressure gradients and differential heating of ice and land from albedo differences can enhance downslope flow (Klein and Heinemann (2002)) and steer it in either direction. The Coriolis force steers in the opposite direction in the southern hemisphere where downslope flow will be -60° to the left and 10° to the right of the AIS topographic

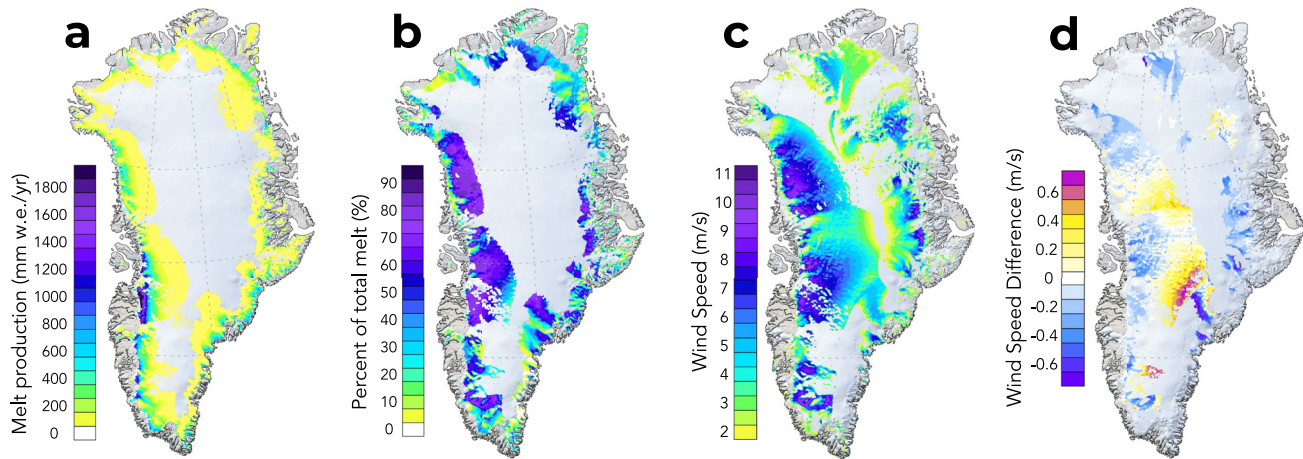


Figure 1. (a) Annual average surface melt pattern when downslope winds are present from 1961 to 2019. (b) Percent of the total melt associated with downslope winds from 1961 to 2019. (c) Average wind speed when downslope winds are present. (d) Multi-decadal difference in wind speed during downslope wind with a statistical significance of 95% computed as 1991–2019 mean minus 1961–1990 mean.

downslope direction. Additionally we do not use slope angle to identify downslope winds because it is important for understanding downslope wind velocity not downslope wind identification. This method does not differentiate katabatic and föhn winds. But is useful for identifying katabatic winds on both ice sheets as well as föhn winds which primarily occur on the AP and Marie Byrd Land of the AIS (Elvidge & Renfrew, 2015; Elvidge et al., 2016; Laffin et al., 2022; Nylan et al., 2004; Speirs et al., 2010). Traditionally, föhn winds are identified by their meteorological signatures of warmth, dryness, direction, and gustiness (Cape et al., 2014; Datta et al., 2019; Elvidge et al., 2020; Laffin et al., 2021; Turton et al., 2018), however this downslope method also identifies föhn winds because on the leeside of the mountains they are funneled through topography as they descend and so mirror topographic slopes (Elvidge et al., 2016).

3. Results

3.1. GIS Downslope Wind Melt Regime

Surface melt associated with the downslope wind direction (accounting for Coriolis steering) occurs primarily on the periphery of the GIS (Figure 1a). Downslope wind-associated surface melt maximizes in the western portion of the ice sheet at $1,910 \pm 5.2$ mm w.e. yr⁻¹, or $64 \pm 5.2\%$ of total melt. Overall, surface melt coincident with downslope winds accounts for $27.5 \pm 4.5\%$ of the total annual surface melt and can reach as high as 98.6% locally (Figure 1b). Most (92.4%) downslope wind-associated melt occurs at lower elevations in the GIS ablation zone, where downslope winds peak and surface temperatures are highest.

The surface energy fluxes that dominate surface melt production associated with downslope winds are shortwave radiation and sensible heat exchange (Wang et al., 2021). Shortwave absorption constitutes $86 \pm 11\%$ of the positive energy balance components during melt associated with downslope flow (Figure S2 in Supporting Information S1). However, this distribution is not uniform over the entire GIS. 79% of the surface melt in the downslope wind-associated melt area on the southern GIS (south of 72°N) is driven by shortwave absorption (>50% of the positive energy balance components), with sensible heat flux (SHF) making up the other 21% (Figure S2a in Supporting Information S1). On the northern portion of the GIS, downslope wind-associated surface melt is primarily driven by the SHF over 70% of the melt area. These results are consistent with Wang et al. (2021) who focused on sub-monthly melt timescales to show that sensible heat drives the melt variability, while we show that shortwave absorption supplies most of the absolute power for total melt.

In the ablation zone on the GIS periphery, where topographic slope and wind speed peak, sensible heat transfers more melt energy to the surface, but does not surpass shortwave absorption as the main driver of melt for the southern GIS (Figure S2 in Supporting Information S1). We also confirm the increase in shortwave absorption and sensible heat during downslope winds when melt occurs (King et al., 2017; Kuipers Munneke et al., 2012, 2018; Wang et al., 2021). However, when melt is absent, downslope winds stronger than 5–9 m/s

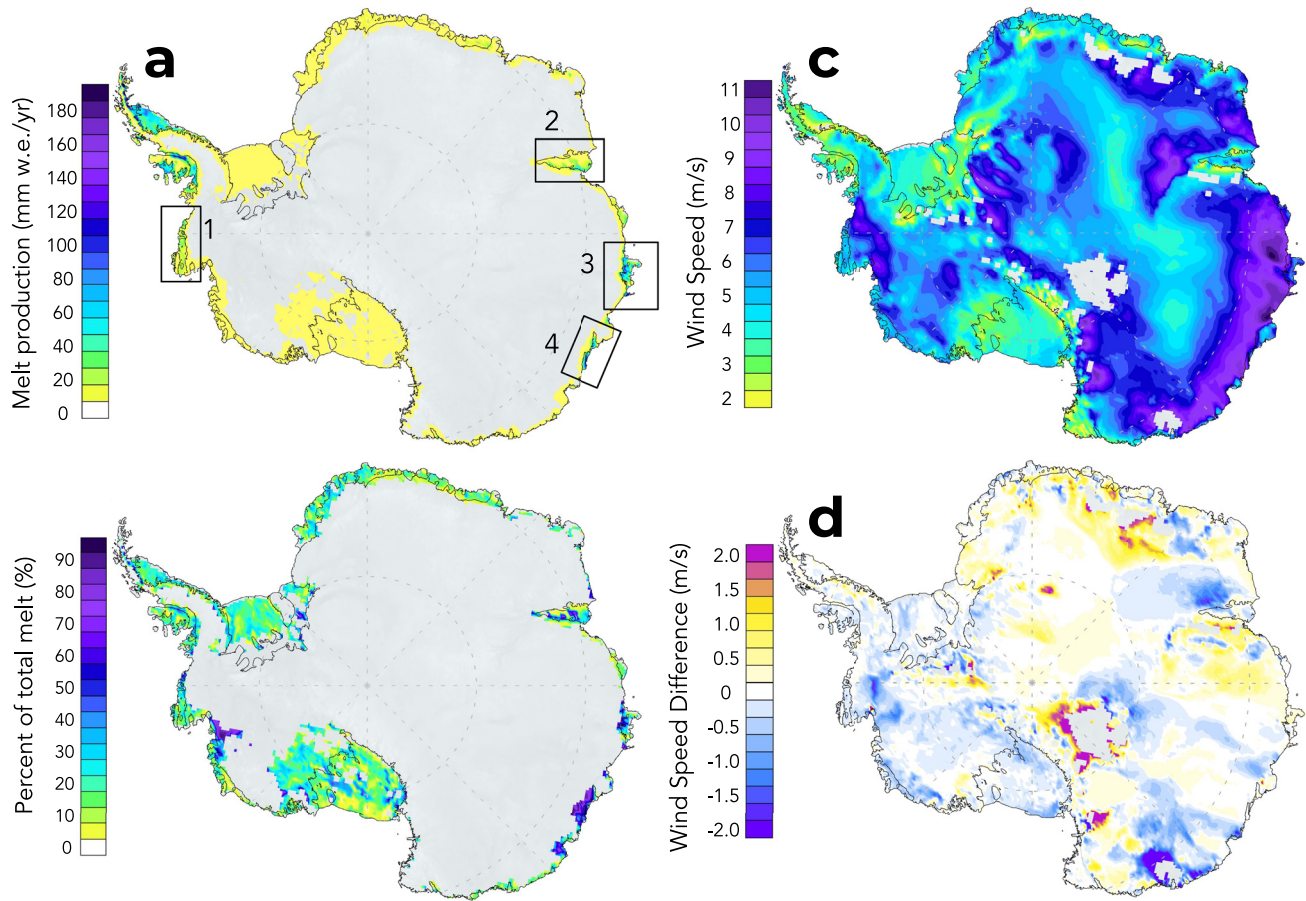


Figure 2. (a) Annual average surface melt pattern when downslope winds are present from 1981 to 2019. Numbered rectangular regions indicate ice shelves; 1-Abbot, 2-Amery, 3-Shackleton, 4-Totten (b) Percent of the total annual melt associated with downslope winds from 1981 to 2019. (c) Average wind speed when downslope winds are present. (d) Difference in wind speed during downslope wind with a statistical significance of 95% from the average of 2001–2019 minus the average of 1981–2000.

(depending on snow type) can create blowing snow that act as low-level clouds that reduce the amount of shortwave absorption at the ice surface (Palm et al., 2017; Xie et al., 2021) (Figure S2b in Supporting Information S1). Additionally, blowing snow also sublimates in the dry katabatic air further reducing air temperature, essentially protecting the ice surface from melt (Palm et al., 2017).

3.2. AIS Downslope Wind Melt Regime

Surface melt associated with the downslope wind direction (steered to the left by the Coriolis effect) occurs primarily on the periphery of the AIS and its ice shelves and constitutes $19.7 \pm 3.8\%$ of total surface melt (Figure 2). The ice shelves (Abbot(1), Amery(2), Shackleton(3), Totten(4)) that often experience katabatic flow also experience enhanced summer surface melt during downslope wind events. Melt associated with downslope winds on Totten and Shackleton ice shelves constitutes $81 \pm 3.7\%$ and $55 \pm 2.5\%$ of their respective total surface melt amounts (Figure 2b). The greatest AIS climatological surface melt rate ($412 \text{ mm w.e. yr}^{-1}$) occurs on the eastern AP due to powerful föhn winds (Cape et al., 2014; Datta et al., 2019; Laffin et al., 2021, 2022). Surface melt is underestimated in this region because the RACMO2 model resolution (27.5 km) does not resolve sub-grid scale föhn winds that are funneled through topography (Laffin et al., 2021). However, this model resolution captures an overall föhn/downslope effect that shows increased surface melt at the base of the AP mountains as observed in previous research (Datta et al., 2019; Elvidge & Renfrew, 2015; Laffin et al., 2021, 2022).

Overall shortwave absorption constitutes $76 \pm 9\%$ of the positive energy balance components during melt associated with downslope flow on the AIS (Figure S4 in Supporting Information S1). This distribution is not uniform

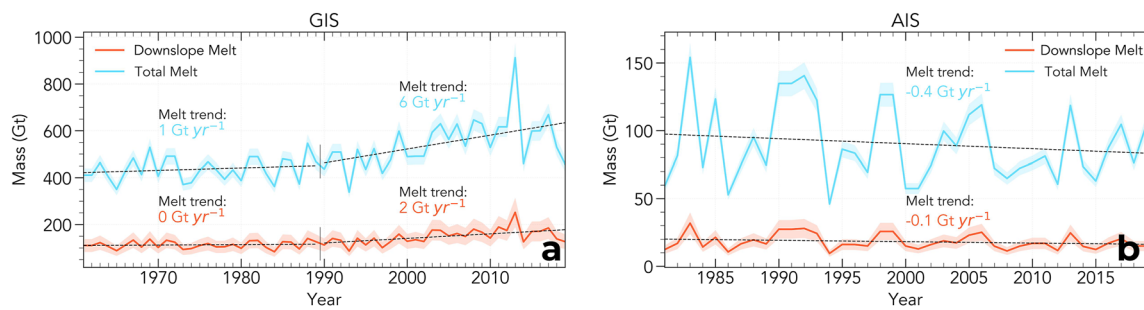


Figure 3. (a) Time series of annual surface melt associated with downslope winds on the GIS from 1961 to 2019. (b) Time series of annual surface melt associated with downslope winds on the Antarctic ice sheets from 1981 to 2019.

over the entire AIS. The surface energy balance, similar to the GIS, also indicates increased solar and sensible heat during melt associated with downslope flow, and reduced shortwave absorption during that does not cause melt likely due to cloud shadowing and to blowing snow that can block shortwave radiation and sublimate (Figure S2 in Supporting Information S1). Nevertheless, the AIS and most of its ice shelves are losing mass at an accelerating rate (Rignot et al., 2013). Warmer atmospheric temperatures and a more positive Southern Annular Mode (SAM) help explain accelerating melt on the AP (Turton et al., 2018).

3.3. Contrasting GIS and AIS Downslope Wind Melt Trends

Surface melt associated with downslope flow on the GIS generally increases through the simulation period (1961–2019), however downslope wind-associated melt increases mainly after the 1990s (Figure 3a; Table S1 in Supporting Information S1). While downslope-associated melt increased by 10.3% from 1991 to 2019 relative to 1961–1990, downslope wind-associated melt did not increase as much compared to total melt (Figure 3a). Prior to the 1990s surface melt associated with downslope winds was stable, however after the 1990s wind-driven melt increased by 14 Gt yr^{-1} ($10.3 \pm 2.5\%$) with the largest increases in June ($1.8\% \text{ yr}^{-1}$) and July ($1.6\% \text{ yr}^{-1}$) (Figure S1 in Supporting Information S1). Over the same period, total surface melt increased by 183 Gt yr^{-1} ($34 \pm 5.8\%$) indicating a reduced role for downslope wind-associated melt as surface temperatures warm, and tend to inhibit downslope wind formation.

The western GIS ablation zone downslope wind speeds slowed on average by 0.37 m/s (6.4%) over the same period (Figure 1d). The North Atlantic Oscillation (NAO) helps explain this apparent conundrum. The negative phase of the summer NAO causes a blocking high to form over the GIS and has become more negative since 1994. This supports the formation of downslope winds and clear skies (Fettweis et al., 2017; Mioduszewski et al., 2016; Tedesco et al., 2013). Negative summer NAO also corresponds with warmer surface temperature that increases surface melt, while inhibiting the formation of downslope winds.

The AIS mean surface melt declined by 5.8 Gt yr^{-1} ($27.8 \pm 5.3\%$) between the periods 1981–2000 and 2001–2019, consistent with previous research on total melt (Figure 3b; Figure S3 in Supporting Information S1) (Trusel et al., 2013). Föhn-winds cause surface melt on the AP that represents $64.3 \pm 6.4\%$ of total AP melt and varies significantly depending on the phase of the SAM and thus drives the AIS-wide melt trend (Laffin et al., 2021, 2022; Turner et al., 2016, 2018). Additionally, increased stratospheric ozone above the AIS has reduced surface insulation and temperatures, hence contributing to the negative melt trend (Abrahamsen et al., 2020; Solomon et al., 2016; Thompson et al., 2011).

4. Discussion and Summary

We use RACMO2 simulations of the GIS from 1961 to 2019 and AIS from 1981 to 2019 to examine how much melt is associated with downslope winds, and how the wind regimes, associated melt, and total melt on each ice sheet have changed. Surface melt associated with downslope winds is significant on both the GIS and AIS, and constitutes a climatological average of 19.7% and 27.5% of total surface melt respectively. The western GIS and AP in particular experience significant melt associated with downslope winds. Overall, the AIS has experienced a reduction of 31.8% in downslope wind-associated melt since 1999 mostly due to reduced föhn generated melt

on the AP (Laffin et al., 2021). The increasing trend in GIS melt associated with downslope winds began in the 1990s with the majority occurring after 2006, however the relative increase in wind-induced melt (10.3%) is smaller than that of total melt (34%). This melt increase is associated with the negative phase of the summer NAO which leads to persistent high pressure blocking over the GIS (Fettweis et al., 2017; Tedesco et al., 2013). The resulting clear skies allow radiative cooling of the ice surface and promote downslope flow. However, the blocking high also increases surface insolation which increases air temperatures and reduces the downslope wind speeds illustrated in Figure 1d. In the ablation zone this blocking has slowed downslope wind speeds yet increased melt because of increased solar surface absorption. In the accumulation zone of the central GIS, winds have accelerated since 1995, likely because the anticyclonic rotation of the blocking high now aligns with the shallow downslope direction and does not indicate an increase in downslope wind strength.

There are clear differences between the GIS and AIS downslope wind associated melt regimes. The relative importance of the positive energy balance components during downslope winds (shortwave absorption (SW) and SHF) differ between the GIS (SW 89%, SHF 11%) and AIS (SW 74%, SHF 26%) for three reasons; (a) the GIS receives more insolation due to its location closer to the equator, (b) the GIS is warmer than the AIS and requires less positive energy balance to trigger melt, (c) the AIS wind-associated melt regime is primarily driven by the AP föhn winds which can significantly enhance sensible heat fluxes compared to katabatic winds (Figure 3b), which are more prominent on the GIS. The GIS wind-associated melt trend has increased by 10.3% in the past 20 years while on the AIS it has decreased by 32%. The wind-associated melt on the AIS has decreased along with total melt, however the variability in AP föhn wind-associated melt in the past 20 years helps explain the total melt decrease, because the majority of surface melt on the AIS occurs on the AP (Turner et al., 2016). In contrast the GIS wind-associated melt regime has increased through time, though more slowly than total surface melt. The enhanced surface temperatures on the GIS reduce the surface air density, increase its buoyancy, and slow the speed of katabatic flow. Total surface melt has increased with higher surface temperatures, despite the slower downslope winds reducing wind-associated melt. This results in a marked contrast between decreasing trends in total and downslope-driven melt on the AIS, and the overall increasing melt trend on the GIS. These results are not surprising considering the ice sheets' locations and temperatures. The GIS trends could be seen as precursors of melt trends that the AIS could experience with continued global warming.

Over the past 20 years downslope wind-associated melt has decreased 31.8% on the AIS while total melt decreased 15.4% due to reduced föhn-induced melt on the AP which drives the overall AIS melt trend. Wind-associated melt has increased by 10.3% on the GIS which is less than the total melt increase of 34%, the result of more negative NAO and summer blocking over the GIS which ultimately leads to warming surface temperatures that reduce downslope wind speeds. In Antarctica, surface melt and subsequent runoff is a key contributor to sea level rise, as it can cause ice shelf instability and halt the buttressing effect on grounded glaciers. Past changes will help clarify how these wind-associated melt regimes will change as the polar regions continue to warm.

Conflict of Interest

The authors declare no conflicts of interest relevant to this study.

Data Availability Statement

RACMO2 model data are available by request at <https://www.projects.science.uu.nl/iceclimate/models>, however, a subset (2001–2018) of the data are hosted online at <https://doi.org/10.5281/zenodo.3677642>. This work utilized the infrastructure for high-performance and high-throughput computing, research data storage and analysis, and scientific software tool integration built, operated, and updated by the Research Cyberinfrastructure Center (RCIC) at the University of California, Irvine (UCI). The RCIC provides cluster-based systems, application software, and scalable storage to directly support the UCI research community. <https://rcic.uci.edu>.

References

- Abrahamsen, E. P., Barreira, S., Bitz, C. M., Butler, A., Clem, K. R., Colwell, S., et al. (2020). Antarctica and the southern ocean. *Bulletin American Meteorology Society*, 101(8), S287–S320. <https://doi.org/10.1175/BAMS-D-20-0090.1>
- Andersen, M. L., Stenseng, L., Skourup, H., Colgan, W., Khan, S. A., Kristensen, S. S., et al. (2015). Basin-scale partitioning of Greenland ice sheet mass balance components (2007–2011). *Earth and Planetary Science Letters*, 409, 89–95. <https://doi.org/10.1016/j.epsl.2014.10.015>

Acknowledgments

MKL was supported by the National Science Foundation (NRT-1633631) and NASA AIST (80NSSC17K0540). CSZ and WW gratefully acknowledges support from the DOE BER ESM and SciDAC programs (DE-SC0019278, LLNL-B641620, LANL-520117). JMVV acknowledges support by PROTECT and was partly funded by the NWO (Netherlands Organisation for Scientific Research) VENI Grant VI.Veni.192.083. BN was funded by the NWO VENI Grant VI.Veni.192.019. We also thank the Institute for Marine and Atmospheric research Utrecht (IMAU) for providing RACMO2 output.

- Auger, M., Morrow, R., Kestenare, E., Sallée, J. B., & Cowley, R. (2021). Southern Ocean in-situ temperature trends over 25 years emerge from interannual variability. *Nature Communications*, *12*(1), 514. <https://doi.org/10.1038/s41467-020-20781-1>
- Bozkurt, D., Bromwich, D. H., Carrasco, J., Hines, K. M., Maureira, J. C., & Rondanelli, R. (2020). Recent near-surface temperature trends in the Antarctic Peninsula from observed, reanalysis and regional climate model data. *Advances in Atmospheric Sciences*, *37*(5), 477–493. <https://doi.org/10.1007/s00376-020-9183-x>
- Bromwich, D. H. (1988). An extraordinary katabatic wind regime at Terra Nova Bay, Antarctica. *Monthly Weather Review*, *117*(3), 688–695. Retrieved from [https://journals.ametsoc.org/doi/abs/10.1175/1520-0493\(1989\)117%3C0688:AEKWRA%3E2.0.CO%3B2](https://journals.ametsoc.org/doi/abs/10.1175/1520-0493(1989)117%3C0688:AEKWRA%3E2.0.CO%3B2)
- Cape, M. R., Vernet, M., Kahru, M., & Spreen, G. (2014). Polynya dynamics drive primary production in the Larsen A and B embayments following ice shelf collapse. *Journal of Geophysical Research: Oceans*, *119*(1), 572–594. <https://doi.org/10.1002/2013JC009441>
- Datta, R. T., Tedesco, M., Fettweis, X., Agosta, C., Lhermitte, S., Lenaerts, J. T. M., & Wever, N. (2019). The effect of foehn-induced surface melt on firn evolution over the northeast Antarctic Peninsula. *Geophysical Research Letters*, *46*(7), 2018GL080845. <https://doi.org/10.1029/2018GL080845>
- Davis, A. M. J., & Mcnider, R. T. (1997). The development of Antarctic katabatic winds and implications for the coastal ocean. *Journal of the Atmospheric Sciences*, *54*(9), 1248–1261. [https://doi.org/10.1175/1520-0469\(1997\)054<1248:tdoakw>2.0.co;2](https://doi.org/10.1175/1520-0469(1997)054<1248:tdoakw>2.0.co;2)
- ECMWF. (2009). IFS documentation CY33R1—Part IV: Physical processes. In *IFS documentation CY33R1* (Vol. 4). <https://doi.org/10.21957/8o7vwlbr>
- Elvidge, A. D., Kuipers Munneke, P., King, J. C., Renfrew, I. A., & Gilbert, E. (2020). Atmospheric drivers of melt on Larsen C Ice Shelf: Surface energy budget regimes and the impact of foehn. *Journal of Geophysical Research: Atmospheres*, *125*(17). <https://doi.org/10.1029/2020JD032463>
- Elvidge, A. D., & Renfrew, I. A. (2015). The causes of foehn warming in the lee of mountains. *Bulletin of the American Meteorological Society*, *97*(3), 455–466. <https://doi.org/10.1175/BAMS-D-14-00194.1>
- Elvidge, A. D., Renfrew, I. A., King, J. C., Orr, A., & Lachlan-Cope, T. A. (2016). Foehn warming distributions in nonlinear and linear flow regimes: A focus on the Antarctic Peninsula. *Quarterly Journal of the Royal Meteorological Society*, *142*(695), 618–631. <https://doi.org/10.1002/qj.2489>
- Enderlin, E. M., Howat, I. M., Jeong, S., Noh, M. J., Van Angelen, J. H., & Van Den Broeke, M. R. (2014). An improved mass budget for the Greenland ice sheet. *Geophysical Research Letters*, *41*(3), 866–872. <https://doi.org/10.1002/2013GL059010>
- Fettweis, X., Box, J. E., Agosta, C., Amory, C., Kittel, C., Lang, C., et al. (2017). Reconstructions of the 1900–2015 Greenland ice sheet surface mass balance using the regional climate MAR model. *The Cryosphere*, *11*(2), 1015–1033. <https://doi.org/10.5194/tc-11-1015-2017>
- Grazioli, J., Madeleine, J. B., Gallée, H., Forbes, R. M., Genthon, C., Krinner, G., & Berne, A. (2017). Katabatic winds diminish precipitation contribution to the Antarctic ice mass balance. *Proceedings of the National Academy of Sciences of the United States of America*, *114*(41), 10858–10863. <https://doi.org/10.1073/pnas.1707633114>
- Hanna, E., Navarro, F. J., Pattyn, F., Domingues, C. M., Fettweis, X., Ivins, E. R., et al. (2013). Ice-sheet mass balance and climate change. *Nature*, *498*(7452), 51–59. <https://doi.org/10.1038/nature12238>
- Hersbach, H., Bell, B., Berrisford, P., Hirahara, S., Horányi, A., Muñoz-Sabater, J., et al. (2020). The ERA5 global reanalysis. *Quarterly Journal of the Royal Meteorological Society*, *146*(730), 1999–2049. <https://doi.org/10.1002/qj.3803>
- Hofer, S., Tedstone, A. J., Fettweis, X., & Bamber, J. L. (2017). Decreasing cloud cover drives the recent mass loss on the Greenland Ice Sheet. *Meteorology*. Retrieved from <https://www.science.org>
- King, J. C., Kirchgassner, A., Bevan, S., Elvidge, A. D., Kuipers Munneke, P., Luckman, A., et al. (2017). The impact of föhn winds on surface energy balance during the 2010–2011 melt season over Larsen C Ice Shelf, Antarctica. *Journal of Geophysical Research: Atmospheres*, *122*(22), 12062–12076. <https://doi.org/10.1002/2017JD026809>
- Klein, T., & Heinemann, G. (2002). Interaction of katabatic winds and mesocyclones near the eastern coast of Greenland. *Meteorological Applications*, *9*(4), 407–422. <https://doi.org/10.1017/S1350482702004036>
- Konrad, H., Shepherd, A., Gilbert, L., Hogg, A. E., McMillan, M., Muir, A., & Slater, T. (2018). Net retreat of Antarctic glacier grounding lines. *Nature Geoscience*, *11*(4), 258–262. <https://doi.org/10.1038/s41561-018-0082-z>
- Kuipers Munneke, P., Luckman, A. J., Bevan, S. L., Smeets, C. J. P. P., Gilbert, E., van den Broeke, M. R., et al. (2018). Intense winter surface melt on an Antarctic Ice Shelf. *Geophysical Research Letters*, *45*(15), 7615–7623. <https://doi.org/10.1029/2018GL077899>
- Kuipers Munneke, P., Van Den Broeke, M. R., King, J. C., Gray, T., & Reijmer, C. H. (2012). Near-surface climate and surface energy budget of Larsen C ice shelf, Antarctic Peninsula. *The Cryosphere*, *6*(2), 353–363. <https://doi.org/10.5194/tc-6-353-2012>
- Laffin, M. K., Zender, C. S., Singh, S., Van Wessem, J. M., Smeets, C. J. P. P., & Reijmer, C. H. (2021). Climatology and evolution of the Antarctic Peninsula föhn wind-induced melt regime from 1979–2018. *Journal of Geophysical Research: Atmospheres*, *126*(4). <https://doi.org/10.1029/2020JD033682>
- Laffin, M. K., Zender, C. S., van Wessem, M., & Marinsek, S. (2022). The role of föhn winds in eastern Antarctic Peninsula rapid ice shelf collapse. *The Cryosphere*, *16*(4), 1369–1381. <https://doi.org/10.5194/tc-16-1369-2022>
- Lenaerts, J. T. M., Lhermitte, S., Drews, R., Ligtenberg, S. R. M., Berger, S., Helm, V., et al. (2017). Meltwater produced by wind-albedo interaction stored in an East Antarctic ice shelf. *Nature Climate Change*, *7*(1), 58–62. <https://doi.org/10.1038/nclimate3180>
- Le Toumelin, L., Amory, C., Favier, V., Kittel, C., Hofer, S., Fettweis, X., et al. (2021). Sensitivity of the surface energy budget to drifting snow as simulated by MAR in coastal Adelie Land, Antarctica. *The Cryosphere*, *15*(8), 3595–3614. <https://doi.org/10.5194/tc-15-3595-2021>
- Massom, R. A., Scambos, T. A., Bennetts, L. G., Reid, P., Squire, V. A., & Stammerjöhn, S. E. (2018). Antarctic ice shelf disintegration triggered by sea ice loss and ocean swell. *Nature*, *558*(7710), 383–389. <https://doi.org/10.1038/s41586-018-0212-1>
- Mattingly, K. S., Turton, J. V., Wille, J. D., Noël, B., Fettweis, X., Rennermalm, Å. K., & Mote, T. L. (2023). Increasing extreme melt in northeast Greenland linked to foehn winds and atmospheric rivers. *Nature Communications*, *14*(1), 1743. <https://doi.org/10.1038/s41467-023-37434-8>
- Mioduszewski, J. R., Rennermalm, A. K., Hammann, A., Tedesco, M., Noble, E. U., Stroeve, J. C., & Mote, T. L. (2016). Atmospheric drivers of Greenland surface melt revealed by self-organizing maps. *Journal of Geophysical Research*, *121*(10), 5095–5114. <https://doi.org/10.1002/2015JD024550>
- Noël, B., van de Berg, W. J., van Wessem, J. M., van Meijgaard, E., van As, D., Lenaerts, J. T. M., et al. (2018). Modelling the climate and surface mass balance of polar ice sheets using RACMO2—Part I: Greenland (1958–2016). *The Cryosphere*, *12*(3), 811–831. <https://doi.org/10.5194/tc-12-811-2018>
- Noël, B., Van De Berg, W. J., Lhermitte, S., & Van Den Broeke, M. R. (2019). Rapid ablation zone expansion amplifies north Greenland mass loss. *Science Advances*, *5*(9). <https://doi.org/10.1126/sciadv.aaw0123>
- Nylan, T. H., Fountain, A. G., & Doran, P. T. (2004). Climatology of katabatic winds in the McMurdo dry valleys, southern Victoria Land, Antarctica. *Journal of Geophysical Research*, *109*(D3), D03114. <https://doi.org/10.1029/2003JD003937>
- Palm, S. P., Kayetha, V., Yang, Y., & Pauly, R. (2017). Blowing snow sublimation and transport over Antarctica from 11 years of CALIPSO observations. *The Cryosphere*, *11*(6), 2555–2569. <https://doi.org/10.5194/tc-11-2555-2017>

- Parish, T. R., & Bromwich, D. H. (1986). The inversion wind pattern over West Antarctica. *Monthly Weather Review*, *114*(5), 849–860. Retrieved from <https://journals.ametsoc.org/doi/10.1175/1520-0493%281986%29114%3C0849%3ATIWP0W%3E2.0.CO%3B2>
- Parish, T. R., & Cassano, J. J. (2003). The role of katabatic winds on the Antarctic surface wind regime. *Monthly Weather Review*, *131*(2), 317–333. [https://doi.org/10.1175/1520-0493\(2003\)131<0317:TROKWO>2.0.CO;2](https://doi.org/10.1175/1520-0493(2003)131<0317:TROKWO>2.0.CO;2)
- Rignot, E., Bamber, J. L., Van Den Broeke, M. R., Davis, C., Li, Y., Van De Berg, W. J., & Van Meijgaard, E. (2008). Recent Antarctic ice mass loss from radar interferometry and regional climate modeling. *Nature Geoscience*, *1*(2), 106–110. <https://doi.org/10.1038/ngeo102>
- Rignot, E., Casassa, G., Gogineni, P., Krabill, W., Rivera, A., & Thomas, R. (2004). Accelerated ice discharge from the Antarctic Peninsula following the collapse of Larsen B ice shelf. *Geophysical Research Letters*, *31*(18), L18401. <https://doi.org/10.1029/2004GL020697>
- Rignot, E., Jacobs, S., Mouginot, B., Scheuchl, B., Wong, M., Conrad, P. G., et al. (2013). Ice-shelf melting around Antarctica. *Science*, *341*(6143), 263–266. <https://doi.org/10.1126/science.1237966>
- Rignot, E., Mouginot, J., Morlighem, M., Seroussi, H., & Scheuchl, B. (2014). Widespread, rapid grounding line retreat of Pine Island, Thwaites, Smith, and Kohler glaciers, west Antarctica, from 1992 to 2011. *Geophysical Research Letters*, *41*(10), 3502–3509. <https://doi.org/10.1002/2014GL060140>
- Scambos, T. A., Bohlander, J. A., Shuman, C. A., & Skvarca, P. (2004). Glacier acceleration and thinning after ice shelf collapse in the Larsen B embayment, Antarctica. *Geophysical Research Letters*, *31*(18), L18402. <https://doi.org/10.1029/2004GL020670>
- Solomon, S., Ivy, D. J., Kinnison, D., Mills, M. J., Neely, R. R., & Schmidt, A. (2016). Emergence of healing in the Antarctic ozone layer. *Science (Washington, DC, United States)*, *353*(6296), 269–274. <https://doi.org/10.1126/science.aae0061>
- Speirs, J. C., Steinhoff, D. F., McGowan, H. A., Bromwich, D. H., & Monaghan, A. J. (2010). Foehn winds in the McMurdo Dry Valleys, Antarctica: The origin of extreme warming events. *Journal of Climate*, *23*(13), 3577–3598. <https://doi.org/10.1175/2010JCLI3382.1>
- Straneo, F., & Heimbach, P. (2013). North Atlantic warming and the retreat of Greenland's outlet glaciers. *Nature*, *504*(7478), 36–43. <https://doi.org/10.1038/nature12854>
- Tedesco, M., Fettweis, X., Mote, T., Wahr, J., Alexander, P., Box, J. E., & Wouters, B. (2013). Evidence and analysis of 2012 Greenland records from spaceborne observations, a regional climate model and reanalysis data. *The Cryosphere*, *7*(2), 615–630. <https://doi.org/10.5194/tc-7-615-2013>
- The IMBIE team. (2020). Mass balance of the Greenland ice sheet from 1992 to 2018. *Nature*, *579*(7798), 233–239. <https://doi.org/10.1038/s41586-019-1855-2>
- Thompson, A. F., Stewart, A. L., Spence, P., & Heywood, K. J. (2018). The Antarctic Slope Current in a changing climate. *Reviews of Geophysics*, *56*(4), 741–770. <https://doi.org/10.1029/2018RG000624>
- Thompson, D., Solomon, S., Kushner, P., England, M. H., Grise, K. M., & Karoly, D. J. (2011). Signatures of the Antarctic ozone hole in Southern Hemisphere surface climate change. *Nature Geoscience*, *4*, 741–749. <https://doi.org/10.1038/ngeo1296>
- Trusel, L. D., Frey, K. E., Das, S. B., Kuipers Munneke, P., & van den Broeke, M. R. (2013). Satellite-based estimates of Antarctic surface meltwater fluxes. *Geophysical Research Letters*, *40*(23), 6148–6153. <https://doi.org/10.1002/2013GL058138>
- Turner, J., Lu, H., White, I., King, J. C., Phillips, T., Hosking, J. S., et al. (2016). Absence of 21st century warming on Antarctic Peninsula consistent with natural variability. *Nature*, *535*(7612), 411–415. <https://doi.org/10.1038/nature18645>
- Turton, J. V., Kirchgassner, A., Ross, A. N., & King, J. C. (2018). The spatial distribution and temporal variability of föhn winds over the Larsen C ice shelf, Antarctica. *Quarterly Journal of the Royal Meteorological Society*, *144*(713), 1169–1178. <https://doi.org/10.1002/qj.3284>
- Van Den Broeke, M. R., & Van Lipzig, N. P. M. (2003). Factors controlling the near-surface wind field in Antarctica *.
- Van Wessem, M. J., Jan Van De Berg, W., Noël, B. P. Y., Van Meijgaard, E., Amory, C., Birnbaum, G., et al. (2018). Modelling the climate and surface mass balance of polar ice sheets using RACMO2—Part 2: Antarctica (1979–2016). *The Cryosphere*, *12*(4), 1479–1498. <https://doi.org/10.5194/tc-12-1479-2018>
- Vihma, T., Tuovinen, E., & Savijrvi, H. (2011). Interaction of katabatic winds and near-surface temperatures in the Antarctic. *Journal of Geophysical Research*, *116*(21), D21119. <https://doi.org/10.1029/2010JD014917>
- Wang, W., Zender, C. S., van As, D., Fausto, R. S., & Laffin, M. K. (2021). Greenland surface melt dominated by solar and sensible heating. *Geophysical Research Letters*, *48*(7), e2020GL090653. <https://doi.org/10.1029/2020GL090653>
- Wenta, M., & Cassano, J. J. (2020). The atmospheric boundary layer and surface conditions during katabatic wind events over the Terra Nova bay Polynya. *Remote Sensing*, *12*(24), 1–32. <https://doi.org/10.3390/rs12244160>
- Xie, Z., Ma, Y., Ma, W., Hu, Z., & Sun, G. (2021). The statistics of blowing snow occurrences from multi-year autonomous snow flux measurements in the French Alps. *The Cryosphere*. <https://doi.org/10.5194/tc-2021-260>